Advanced Composite Materials
Publication details, including instructions for authors and subscription information:
http://www.tandfonline.com/loi/tacm20

Measurement of dynamic interlaminar fracture toughness of FRP laminates using dynamic displacement measuring apparatus

Mitsugu Todo [a], Takashige Nakamura [b], Toshio Mada [c] & Kiyoshi Takahashi [d]

[a] Research Institute for Applied Mechanics, Kyushu University, Kasuga, Fukuoka 816, Japan

[b] Research Institute for Applied Mechanics, Kyushu University, Kasuga, Fukuoka 816, Japan

[c] Research Institute for Applied Mechanics, Kyushu University, Kasuga, Fukuoka 816, Japan

[d] Research Institute for Applied Mechanics, Kyushu University, Kasuga, Fukuoka 816, Japan

Version of record first published: 02 Apr 2012.

To cite this article: Mitsugu Todo , Takashige Nakamura , Toshio Mada & Kiyoshi Takahashi (1998): Measurement of dynamic interlaminar fracture toughness of FRP laminates using dynamic displacement measuring apparatus, Advanced Composite Materials, 7:3, 285-297

To link to this article: http://dx.doi.org/10.1163/156855198X00200

Adv. Composite Mater., Vol. 7, No. 3, pp. 285–297 (1998)

JSCM Award Winning Paper

Measurement of dynamic interlaminar fracture toughness of FRP laminates using dynamic displacement measuring apparatus

MITSUGU TODO *, TAKASHIGE NAKAMURA, TOSHIO MADA and KIYOSHI TAKAHASHI

Research Institute for Applied Mechanics, Kyushu University, Kasuga, Fukuoka 816, Japan

Abstract—Dynamic mode II and mixed-mode interlaminar fracture toughnesses of CFRP laminates were measured using an instrumented impact testing system at a low impact speed (0.9 m/s). The system consisted of an instrumented drop weight impact tester and dynamic displacement measuring apparatus constructed from an optical fiber, position sensing detector and laser light source. The results showed that if dynamic interlaminar fracture toughness is estimated on the basis of load data obtained from a strain gage signal measured on the falling dart, the dynamic toughness could be overestimated, resulting in an erroneous understanding of the experimental results. It was also shown that the dynamic toughness can be evaluated accurately on the basis of the displacement data measured by the dynamic displacement measuring apparatus. It is thus concluded that the displacement-based analysis is more accurate and reliable than the load-based analysis in the measurement of the dynamic interlaminar fracture toughness of FRP laminates.

Keywords: Delamination; interlaminar fracture toughness; loading rate effect; impact testing; CFRP laminates.

1. INTRODUCTION

Fiber reinforced plastics (FRP) have been used as structural materials in a wide variety of engineering fields. It has been known that interlaminar fracture tends to be easily generated in FRP laminates that possess relatively low interlaminar strength compared to high strength in the fiber direction. Therefore, many attempts have been made to evaluate the interlaminar fracture toughness of FRP laminates quantitatively, and testing standards have been developed for static interlaminar fracture tests [1, 2]. It has also been known that significant delaminations may

*To whom correspondence should be addressed.

be generated in FRP structures when they are subjected to dynamic loads. We, therefore, need to understand the effects of loading rate on the interlaminar fracture resistance of FRP laminates. However, reliable testing methods for the measurement of dynamic interlaminar fracture toughness have not been established yet, and the rate effects on the interlaminar fracture toughness are not well understood [3].

Few attempts have been made to estimate the dynamic mode II interlaminar fracture toughness of FRP laminates. In these studies, a hydraulic testing machine (loading rates of less than 0.1 m/s) [4], a drop weight testing system (1.25 to 3 m/s) [5, 6], and the split Hopkinson pressure bar (SHPB) method (0.2 to 20 m/s) [7–9] were utilized in dynamic mode II interlaminar fracture tests. In the instrumented drop weight testing system, it is usually difficult to evaluate the load applied to the specimen accurately because periodic oscillation due to inertial effect and the multiple-reflection of the stress wave is normally observed in the load–time history when the load is measured from strain gages attached to the loading dart [10]. Since loading-point displacement is usually evaluated from the load data by assuming the loading dart as a rigid body, the obtained load–displacement relation at the loading point and absorbed impact energy calculated from the relation may not be accurate enough. On the other hand, the SHPB method enables one to conduct dynamic tests at higher loading rates than the drop weight system with relatively accurate measurement of the load because there is no effect of stress wave reflection on the load data. However, displacement data may not be accurate enough because it is indirectly evaluated from strain gage signals measured on the input and output bars. To overcome such problems related to the displacement measurement in those dynamic testings, our research group has recently developed a dynamic displacement measuring apparatus, and applied it to the study of the dynamic behaviors of polymers and polymeric composites [11, 12].

In this study, the dynamic mode II and mixed-mode interlaminar fracture toughness of carbon fiber reinforced plastics (CFRP) were measured using an impact testing system consisting of an instrumented drop weight impact testing machine and the dynamic displacement measuring apparatus. Then, the validity of the dynamic toughness evaluation on the basis of directly measured displacement was discussed.

2. EXPERIMENTAL

2.1. Specimen

Two kinds of CFRP laminates, T800H/2500 and T800H/3631, were investigated in this study. The 2500 is a 120°C cured epoxy resin, and 3631 a 180°C cured thermoplastic modified epoxy resin. Laminate configuration was $[0^\circ_{20}]$ and Kapton film was inserted between the middle layers to introduce an artificial delamination. Initial crack was introduced using a fresh razor blade prior to the testing. End

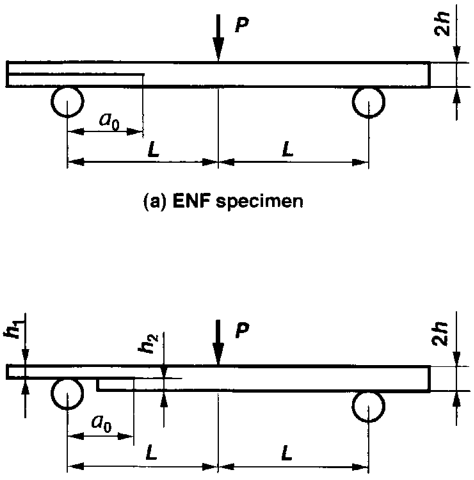

Figure 1. Interlaminar fracture test specimens. For ENF specimen, $a_0 = 25$, $L = 50$, $2h = 2.7$ and the width $B = 12$ (mm). For MMF specimen, $a_0 = 30$ (25 for dynamic test), $L = 60$ (50 for dynamic test), $2h = 2.7$, $h_1 = h_2$ and the width $B = 12$ (mm).

notched flexure (ENF) specimen for mode II test and mixed-mode flexure (MMF) specimen for mixed-mode (mode I + mode II) test are shown in Fig. 1. Both ENF and MMF testings were performed under three-point bending loading condition. The ratio of mode I to mode II in MMF specimen can be varied by changing the ratio h_1/h_2 (see Fig. 1b) [13–15].

2.2. *Static interlaminar fracture test*

Static mode II and mixed-mode interlaminar fracture tests were performed using a servohydraulic testing machine at a quasi-static loading rate of 0.5 mm/min. Three-point bending tests were conducted and load–displacement curves were recorded.

2.3. *Dynamic interlaminar fracture test*

Dynamic interlaminar fracture tests were performed at a low impact speed of 0.9 m/s using the dynamic testing system consisting of a drop weight testing machine and dynamic displacement measuring apparatus. The dynamic testing system is shown in Fig. 2. Load data is obtained from the output of strain gages attached to the loading dart, and load calibration is done statically by changing the weight of the dart. In a standard drop weight testing, periodic oscillation is generally observed on the load data. This kind of dynamic effect can be reduced by placing a viscoelastic sheet on the loading-point of the specimen [16]. In this study, a rubber sheet of 1.5 mm thick was used to reduce the dynamic effect.

The dynamic displacement measuring apparatus newly developed consists of an optical fiber, He-Ne laser, position sensing detector (PSD) sensor and an

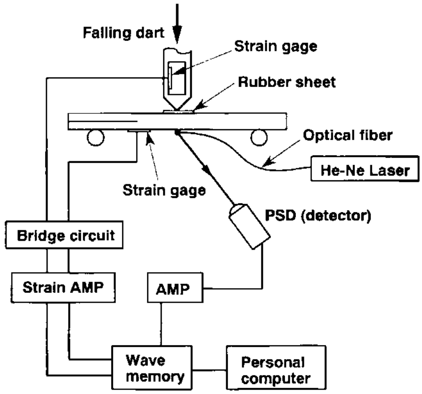

Figure 2. Dynamic testing system consisting of drop weight impact tester and dynamic displacement measuring apparatus.

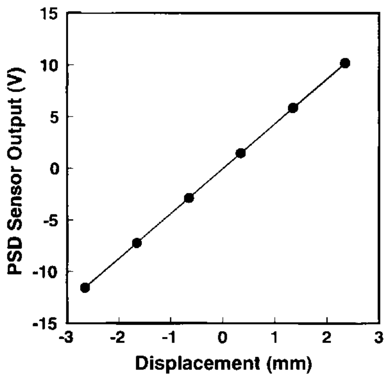

Figure 3. Relation between PSD sensor output and displacement.

amplifier [12]. An end of the optical fiber is attached to the specimen surface just underneath the loading point, and laser light is introduced into the optical fiber from the other end. The laser light coming from the edge of the optical fiber placed on the specimen surface is concentrated through an optical lens and received by the PSD. The output of the PSD is sent to a personal computer through the amplifier and wave memory. The position of the PSD can be changed by micrometer, and displacement calibration is conducted by moving the PSD in the direction of deflection. The linear relation between the PSD output and displacement is shown in Fig. 3.

In standard instrumented drop weight testing systems, deflection at the loading-point of the specimen is generally evaluated indirectly on the basis of the change of acceleration of the loading dart [17]. Acceleration A, velocity V, distance of the movement D of the dart at time t after collision between the dart and specimen are given by

$$A(t) = P(t)/m - g, \tag{1}$$

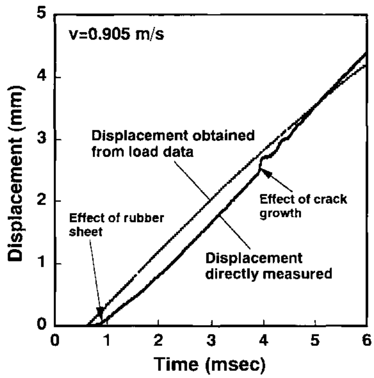

Figure 4. Loading-point displacements for an ENF specimen of T800H/2500 obtained from dynamic displacement measuring apparatus and strain gage signal from loading dart.

$$V(t) = V_0 - \int_{t_0}^{t} A\,\mathrm{d}t, \tag{2}$$

$$D(t) = \int_{t_0}^{t} V\,\mathrm{d}t, \tag{3}$$

where P is the load, m the weight of the dart, g the gravitational acceleration and t_0 the starting time of the collision. The velocity V_0 of the dart at the collision is given by $V_0 = \sqrt{2gh}$, where h is the drop height of the dart. As an example of ENF test results, displacement data obtained from the dynamic displacement measuring apparatus and the analytical method described above are shown in Fig. 4. It should be noted that the displacement directly measured exhibits slow increase at initiation, which is considered to be an effect of the rubber sheet, and sudden increase caused by the reduction of stiffness due to interlaminar crack growth. It thus appears that it is possible to evaluate displacement more accurately using the dynamic displacement measuring apparatus than the analytical method.

Strain on the surface of the specimens close to the initial crack tip was measured to detect the initiation of crack growth. Based upon the finite element analysis, Kusaka *et al.* revealed that the strain on the specimen surface shows a dramatic change due to the initiation of crack growth [18]. It thus appears that a crack initiation can be detected from the change of strain observed in the measured strain–time curve. For ENF specimens, the strain gage was attached to a point close to the crack tip on the bottom surface, where tensile strain was generated. On the other hand, for MMF specimens, the strain gage was attached to the top surface, where compressive strain was generated.

The sampling interval was 1 μs for all measured data including load, displacement and strain on the specimen surface.

3. EVALUATION OF MODE II INTERLAMINAR FRACTURE TOUGHNESS

3.1. Static interlaminar fracture toughness

Mode II interlaminar fracture toughness G_{IIC} at a crack initiation can be expressed as [1]:

$$G_{IIC} = \frac{9a_1^2 P_C^2 C_1}{2B(2L^3 + 3a_1^3)}, \tag{4}$$

where P_C is the critical load, C_1 the compliance at P_C, B the width of the specimen, and L the span length; a_1 is an estimated crack length at P_C and given by:

$$a_1 = \left[\frac{C_1}{C_0}a_0^3 + \frac{2}{3}\left(\frac{C_1}{C_0} - 1\right)L^3\right]^{1/3}, \tag{5}$$

where C_0 and a_0 are the initial compliance and the crack length of the specimen, respectively.

Mixed-mode interlaminar fracture toughness G_C is given by [14]:

$$G_C = \frac{21a_0^2 P_C^2 C_0}{2B(2L^3 + 7a_0^3)}. \tag{6}$$

Using classical beam theory, for the MMF specimen used in this study, the mode I and mode II contributions to the G_C can be expressed as [19]:

$$G_I = \frac{6a^2 P^2}{B(2L^3 + 7a^3)}, \qquad G_{II} = \frac{9a^2 P^2}{2B(2L^3 + 7a^3)}. \tag{7}$$

Using equation (7), the mode I contribution in the present MMF testing can be estimated approximately as 57%.

3.2. Dynamic interlaminar fracture toughness

In dynamic testings, specimens generally tend to oscillate periodically as a result of impact, and the deformation and stress states of the specimens are different from those under static loading conditions. Therefore, dynamic effects must be considered in the analysis of dynamic test results. In this study, it was reasonably assumed that dynamic effects were negligibly small so that quasi-static stress states were achieved, since the dynamic tests were performed at a low rate of 0.9 m/s, and a piece of rubber sheet was used for mechanical filtering. Thus, the equations developed for the static analyses were used for estimating the dynamic interlaminar fracture toughnesses. If it is assumed that any subcritical crack growth does not occur prior to the crack initiation, equation (4) becomes:

$$G_{IIC} = \frac{9a_0^2 P_C^2 C_0}{2B(2L^3 + 3a_0^3)}. \tag{8}$$

The compliance C_0 for an ENF specimen is given by [20]:

$$C_0 = \frac{2L^3 + 3a_0^3}{8EBh^3}, \tag{9}$$

where E and $2h$ are the bending modulus and the thickness of the specimen, respectively. Substitution of equation (9) into equation (8) yields:

$$G_{\mathrm{IIC}} = \frac{9a_0^2 P_\mathrm{C}^2}{16EB^2h^3}. \tag{10}$$

Using the relation $P_\mathrm{C} = \delta_\mathrm{C}/C_0$ with equation (9), equation (8) becomes

$$G_{\mathrm{IIC}} = \frac{36a_0^2 \delta_\mathrm{C}^2 Eh^3}{\left(2L^3 + 3a_0^3\right)^2}, \tag{11}$$

where δ_C is the critical deflection corresponding to the critical load P_C. In this study, equation (10) was used instead of equation (8), since it was difficult to measure the compliance C_0 accurately in the dynamic tests due to the oscillation that appeared in the measured data. By assuming that the modulus E at the low loading rate (0.9 m/s) is the same as that at static loading rates, the average of E values obtained from the static tests was used in the dynamic analysis. Equation (11) was also used for the comparison between the load-based analysis (equation (10)) and the deflection-based analysis (equation (11)).

Dynamic mixed-mode interlaminar fracture toughness was estimated using the static equation (6). The compliance for MMF specimen is given by [14]:

$$C_0 = \frac{2L^3 + 7a_0^3}{8EBh^3}. \tag{12}$$

Substitution of equation (12) into equation (6) yields:

$$G_\mathrm{C} = \frac{21a_0^2 P_\mathrm{C}^2}{16EB^2h^3}. \tag{13}$$

Using the relation $P_\mathrm{C} = \delta_\mathrm{C}/C_0$ with equation (12), equation (6) becomes:

$$G_\mathrm{C} = \frac{84a_0^2 \delta_\mathrm{C}^2 Eh^3}{\left(2L^3 + 7a_0^3\right)^2}. \tag{14}$$

Dynamic mixed-mode interlaminar fracture toughness was estimated using equation (13) or equation (14). The static value of E was used in the dynamic mixed-mode analysis.

4. RESULTS AND DISCUSSION

4.1. Static interlaminar fracture toughness

Examples of the load–displacement curves obtained from the static ENF and MMF tests are shown in Fig. 5. For the ENF tests, P_C, C_0 and C_1 were evaluated from

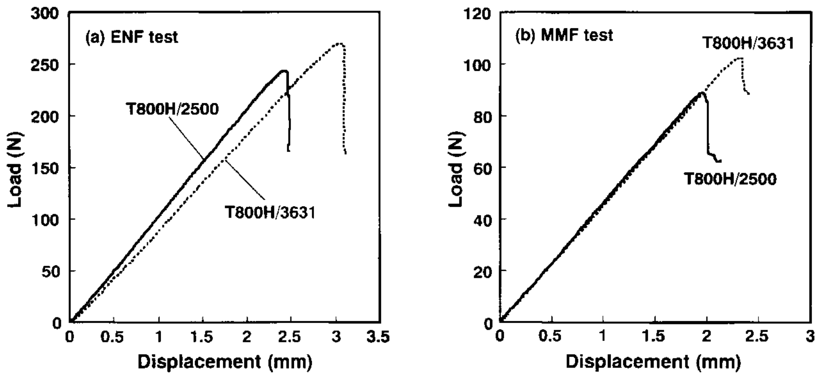

Figure 5. Load–displacement curves obtained from static interlaminar fracture tests: (a) ENF test; (b) MMF test.

Table 1.
Static and dynamic mode II interlaminar fracture toughnesses of CFRP laminates

	Static	Dynamic			
	G_{IIC} (J/m^2)	G_{IIC} (P_A) (J/m^2)	G_{IIC} (δ_A) (J/m^2)	G_{IIC} (P_B) (J/m^2)	G_{IIC} (δ_B) (J/m^2)
T800H/2500	534	533	467	599	482
T800H/3631	727	612	596	717	615

Table 2.
Static and dynamic mixed-mode interlaminar fracture toughnesses of CFRP laminates

	Static	Dynamic			
	G_C (J/m^2)	G_C (P_A) (J/m^2)	G_C (δ_A) (J/m^2)	G_C (P_B) (J/m^2)	G_C (δ_B) (J/m^2)
T800H/2500	226	219	196	271	245
T800H/3631	303	284	245	310	291

the load–displacement curves on the basis of JIS K 7086 [1]. For the MMF tests, the maximum load was simply chosen as P_C. The static mode II and mixed-mode interlaminar fracture toughnesses evaluated using equations (4) and (6), respectively, are shown in Tables 1 and 2.

4.2. Dynamic interlaminar fracture toughness

Examples of the load and displacement–time curves obtained from the dynamic interlaminar fracture tests of T800H/2500 are shown in Fig. 6. The strain gage signal measured on the specimen surface close to the crack tip is also shown in each figure. For both the ENF and MMF tests, slight oscillations were observed on the

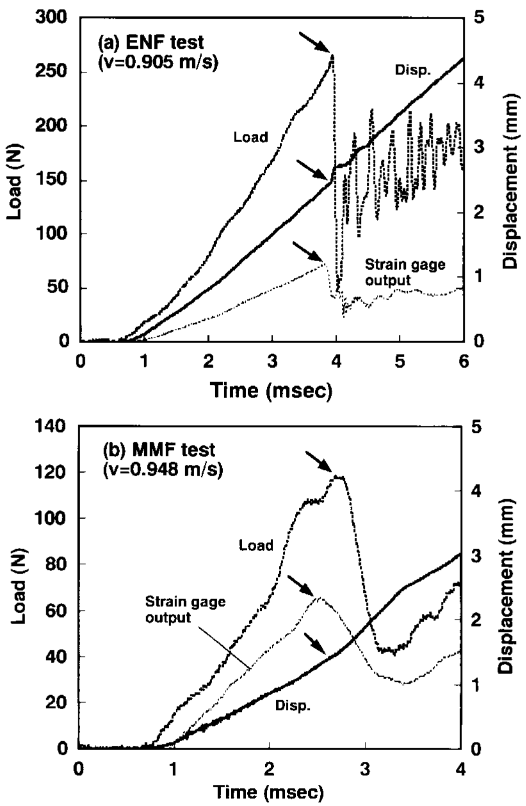

Figure 6. Load and displacement–time curves for T800H/2500 obtained from dynamic interlaminar fracture tests. Strain gage signals measured on the specimen surface close to the crack tip are also shown in the figures. The arrows indicate the critical points corresponding to crack initiation: (a) ENF test; (b) MMF test.

load–time curves. Sudden decreases of the load and the strain gage signal were also seen just after they reached their maximums in the figures. It is considered that these decreases were caused by initiation of the crack. On the other hand, the displacement exhibited slight increase at the crack initiation as a result of the decreasing stiffness of the specimens. The inflection points corresponding to these changes occurred in the order of the strain gage signal, the displacement and the load. For the ENF test, for example, the inflection points on the displacement and load curves delayed about 70 μs and 100 μs, respectively, from the inflection point on the strain gage signal. Thus, the strain gage signal, which was measured at the closest point to the crack tip, indicated the fastest response to the crack initiation.

Maximum load value has been generally accepted as a critical load corresponding to the crack initiation and this has been used for estimating the dynamic interlaminar fracture toughness of brittle FRPs. In this study, however, both critical load and critical displacement were used for evaluating the interlaminar fracture toughnesses. These critical values were determined by using the two different methods on the basis of the inflection points appearing on the three curves, that is, the load, displacement and strain gage signal–time curves. The methods are as follows:

(A) The critical load and displacement are estimated at the time of the maximum of the strain gage signal. The critical values are denoted by P_A and δ_A, respectively.

(B) The critical load and displacement are obtained at the inflection points of the load and displacement–time curves, respectively. These values are denoted by P_B and δ_B, respectively.

For both the ENF and MMF tests, the inflection points appearing on the displacement–time curves were determined by analyzing the velocity of the specimen at the loading-point which can be obtained by differentiating the loading-point displacement numerically with respect to time. The inflection points on the displacement–time curves can be found as the points at which the velocity indicates sudden increase, as shown in Fig. 7.

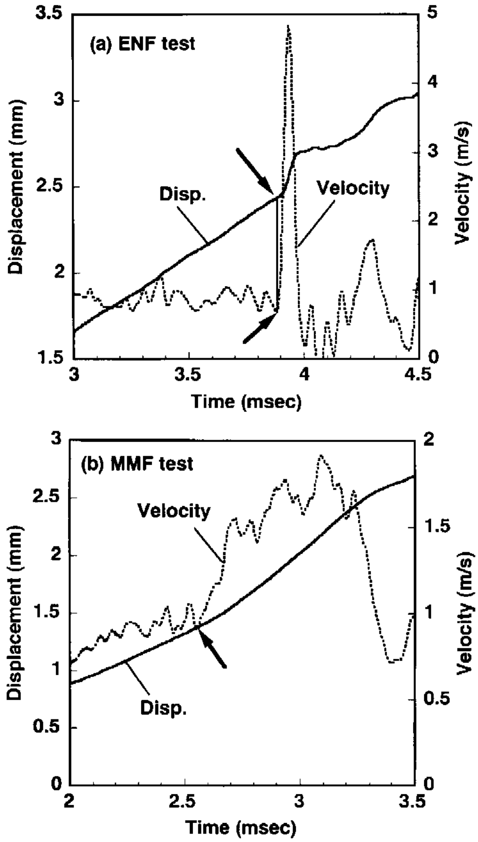

Figure 7. Displacement and velocity–time curves for T800H/2500 obtained from dynamic interlaminar fracture tests. The arrows indicate the critical points corresponding to crack initiation: (a) ENF test; (b) MMF test.

The dynamic mode II interlaminar fracture toughness evaluated using equations (10) and (11) and dynamic mixed-mode interlaminar fracture toughness evaluated using equations (13) and (14) are shown in Tables 1 and 2, respectively. From these tables, it can be seen that all the dynamic toughness values obtained on the basis of the A method were lower than the static ones. Thus, the interlaminar fracture toughnesses tend to decrease as loading rate increases. On the other hand, among the dynamic toughness values evaluated on the basis of the B method, G_{IIC} (P_B), G_C (P_B) and G_C (δ_B), of T800H/2500 and G_C (P_B) of T800H/3631 were higher than the static ones. This implies that the rate dependence on the interlaminar fracture toughness could be understood differently, depending upon how the critical values of load or displacement are estimated. This indicates that a definite tendency for the rate dependence on the interlaminar fracture toughness of FRP laminates has not been obtained yet. All the interlaminar fracture toughness values estimated on the basis of load were higher than those estimated on the basis of displacement. It appears that this is because the critical load values were over-estimated due to the effect of oscillation on the load data. These results suggest that it is very important that the initiation point of crack growth is estimated accurately in the dynamic interlaminar fracture tests. It appears that the proposed method (the method A), in which the crack initiation point is determined from the strain gage signal measured on the specimen surface and then the interlaminar fracture toughness is evaluated on the basis of the loading-point displacement measured using the dynamic displacement measuring apparatus, is a reasonable way to evaluate the dynamic interlaminar fracture toughness of FRP laminates accurately.

In the present study, only static equations were used for estimating the dynamic interlaminar fracture toughnesses. However, dynamic effects must be included in the analysis of the dynamic interlaminar fracture testing results performed at higher rates of loading [21, 22]. On the other hand, it has been shown that it is possible to apply the static analyses to the dynamic testings even at relatively high rates if quasi-static stress states are achieved [7–9]. Application of the dynamic displacement measuring apparatus to such kinds of high speed testing will be considered in the near future.

5. CONCLUSIONS

Dynamic mode II and mixed-mode interlaminar fracture tests were performed using a newly developed dynamic testing system consisting of an instrumented drop weight testing machine and dynamic displacement measuring apparatus. Applicability of the new dynamic testing system was discussed, and the following conclusions were obtained.

(1) It is possible to measure the loading-point displacement relatively easily and accurately using the newly developed dynamic displacement measuring

apparatus, and the dynamic interlaminar fracture toughness can be evaluated on the basis of the directly measured displacement.

(2) If the dynamic interlaminar fracture toughness is evaluated on the basis of the load data measured by strain gages attached to the loading dart, overestimation of the toughness could happen due to the dynamic effects appearing on the load data.

(3) The initiation of crack growth can be detected from the strain gage signal measured on the specimen surface close to the crack tip, and the dynamic interlaminar fracture toughness can be evaluated accurately on the basis of the critical displacement corresponding to the initiation.

Acknowledgements

The authors would like to thank Dr. Philippe Béguelin (EPFL, Switzerland) for assistance in the development of the dynamic displacement measuring apparatus. The authors would also like to acknowledge Toray Industries Inc. for providing the materials.

REFERENCES

1. Testing methods for Interlaminar Fracture Toughness of Carbon Fibre Reinforced Plastics, JIS K 7086-1993, Japanese Industrial Standards Group (1993).
2. Standards Test Method for Mode I Interlaminar Fracture Toughness of Unidirectional Reinforced Polymer Matrix Composites, ASTM Standard D5228-94, DCB Standard, American Society for Testing and Materials (1994).
3. M. Tohdoh, S. K. Chaturvedi and R. L. Sierakowski, Dynamic interlaminar fracture toughness of composite laminates: A review, in: *Proc. of the Sixth Japan–US Conference on Composite Materials*, pp. 694–702 (1992).
4. A. J. Smiley and R. B. Pipes, Rate sensitivity of mode II interlaminar fracture toughness in graphite/epoxy and graphite/PEEK composite materials, *Comp. Sci. Tech.* **29**, 1–15 (1987).
5. H. Maikuma, J. W. Gillespie, Jr. and D. J. Wilkins, Mode II interlaminar fracture of the center notch flexural specimen under impact loading, *J. Comp. Mater.* **24**, 124–149 (1990).
6. K. Kageyama, I. Kimpara, T. Suzuki, I. Ohsawa and S. Kabashima, Mode II interlaminar fracture toughness under impact loading, in: *Proc. of 'Benibana' Inter. Symp. on How to Improve the Toughness of Polymers and Composites*, pp. 190–194 (1990).
7. Y. Yamauchi, T. Kurokawa and T. Kusaka, Estimation of dynamic interlaminar fracture toughness of CFRP by ENF test using SHPB method, *J. Soc. Mat. Sci., Japan* **42**, 1445–1451 (1993).
8. T. Kusaka, T. Kurokawa and Y. Yamauchi, Strain rate dependence of mode II interlaminar fracture toughness of unidirectional CF/epoxy composite laminates, *J. Soc. Mat. Sci., Japan* **43**, 445–450 (1994).
9. T. Kusaka, T. Kurokawa, M. Hojo and S. Ochiai, Finite element simulation of impact end notched flexure test using ramped incident waves, *Trans. of the Japan Soc. of Mech. Eng.* **A63**, 158–164 (1997).
10. M. C. Cheresh and S. McMichael, Instrumented impact test data interpretation, in: *Instrumented Impact Testing Plastics and Composite Materials, ASTM STP 936*, pp. 9–23. American Society for Testing and Materials, Philadelphia (1987).

11. T. Nakamura, M. Todo and K. Takahashi, Measurement of dynamic mode II and mixed-mode interlaminar fracture toughness of CFRP laminates, in: *Proc. JSMS Composites-26*, pp. 43–46 (1997).
12. T. Mada, K. Takahashi, Ph. Beguelin and G. Aggag, Construction of a dynamic displacement measurement apparatus and its application to impact fracture studies, *Trans. of the Japan Soc. of Mech. Eng.* **A63**, 71–76 (1997).
13. S. H. Yoon and C. S. Hong, Modified end notched flexure specimen for mixed mode interlaminar fracture in laminated composites, *Inter. J. Fracture* **43**, R3–R9 (1990).
14. C. S. Hong and J. Y. Shim, Evaluation of strain energy release rates of mixed-mode fracture specimen for laminated composites, in: *Proc. 9th Intern. Conf. on Composite Materials*, Vol. V, pp. 779–786 (1993).
15. B. D. Davidson, R. Kruger and M. Konig, Three-dimensional analysis of center-delaminated unidirectional and multidirectional single-leg bending specimens, *Comp. Sci. Tech.* **54**, 385–394 (1995).
16. G. Aggag and K. Takahashi, Study of oscillation signals in instrumented Charpy impact testing, *Polym. Engng Sci.* **36**, 2260–2266 (1996).
17. I. Narisawa, M. Ishikawa and K. Sato, Instrumented Charpy impact test of polymers, *Kobunshi Ronbunshu* **44**, 845–852 (1987).
18. T. Kusaka, T. Kurokawa, M. Hojo and S. Ochiai, Estimation of interlaminar fracture toughness of CFRP laminates by measuring the surface strain of specimen, in: *Proc. JSMS Composites-26*, pp. 203–204 (1996).
19. J. G. Williams, On the calculation of energy release rates for cracked laminates, *Inter. J. Fracture* **36**, 101–119 (1988).
20. L. A. Carlsson and R. B. Pipes, *Experimental Characterization of Advanced Composite Materials*. Prentice Hall, New Jersey (1987).
21. N. Sakabe, T. Adachi and H. Matsumoto, Approximate analysis of J-integral for dynamic ENF test of FRP, in: *Proc. 1994 Annual Meeting of JSME/MMD*, Vol. B, pp. 246–247 (1994).
22. M. Arai, T. Kobayashi, T. Adachi and H. Matsumoto, Evaluation of dynamic fracture toughness of unidirectional CFRP laminates, in: *Proc. 1996 Annual Meeting of JSME/MMD*, Vol. A, pp. 331–332 (1996).